THE ASTROPHYSICAL JOURNAL, **234**:275–288, 1979 November 15

A METHOD FOR SOLVING BINARY STAR ORBITS USING THE FOURIER TRANSFORM

DAVID G. MONET
Yerkes Observatory
Received 1979 May 7; accepted 1979 June 5

ABSTRACT

This paper details the solutions of binary star orbits based on the Fourier transform of the equations of motion. The method has the advantages of a least-squares fit to the weighted observations, noniterative and impersonal solution of the exact equations, and adequate error analysis. The method is applied to spectroscopic and visual binary systems. In addition, it allows for the solution of an orbit based on the position angles and separations separately. The relevant equations for each of the four cases are presented. An algorithm for the implementation of each solution is discussed. Sample orbits were calculated by the Fourier transform method, and the results are compared, when possible, with previously published orbits for the same systems.

Subject headings: functions: numerical methods — stars: binaries — stars: visual multiples

I. INTRODUCTION

The purpose of this paper is to present relevant equations involved in the use of the Fourier transform in the computation of binary star orbits, and to discuss some aspects of their implementation. The discussion is limited to cases of orbital eccentricity e less than unity. The remaining portion of this section discusses the desirability of this approach to the problem and its advantages in comparison with the plethora of other methods available. Section II presents equations concerning the computed Fourier transform of Kepler motion seen in four astronomical contexts: the spectroscopic binary, the visual binary, the visual binary when no information concerning separations is available, and the visual binary when no information concerning the position angle is available. In addition, algorithms for computing the orbital elements are presented for each of these cases. Section III is devoted to some of the complexities which arise in the implementation of the theoretical results derived in § II. Section IV presents a general discussion of the method and some conclusions that may be drawn.

Before discussing particular manifestations of orbit determination theory, it is important to phrase the problem in its observational context. For a particular system, one has a finite number of observations, each having some relative weight, and the hypothesis of Kepler motion is presumed. The analysis procedure must address the following concerns: (1) whether Kepler motion is a justifiable hypothesis, or whether the data is adequately represented by some simpler hypothesis in combination with observational uncertainty; and (2) whether Kepler motion is an adequate hypothesis, or whether additional effects, such as apsidal motion, unseen companions, etc., need be introduced. The observations contain components of signal, which is the systematic variation of the observable quantity, and noise, which is the unavoidable contribution of observational uncertainty. The orbit determination problem is then to determine the best (in some specified context) estimator of the signal in the presence of the noise, and to measure the uncertainty in the determined properties of the signal due to the noise.

The role of the theory developed in § II is to determine the properties of the signal due to Kepler motion. The orbital elements which describe Kepler motion fall into three distinct groups. The first is the periodicity of the motion. Kepler orbits are a particular subset of periodic functions, and hence procedures must exist for determining the periodicity which make no reference to the Kepler hypothesis. Ideally, the orbital period should be determined in such a manner, and the orbital analysis, which introduces the Kepler motion hypothesis, should be done at fixed period. In practice, the orbital period may be determined in the manner described in § III. The second group of orbital elements are those dealing with scale and orientation in space. The observed amplitude of motion is related by a constant to an ellipse of unit semimajor axis. The elements Ω, i, and ω are simply related to the Euler rotation matrix angles (ϕ, θ, and ψ, respectively, in the notation of Goldstein 1950). If the other elements are known, these may be directly measured in either configuration or transform space. The third group consists of the eccentricity e and the time of periastron passage T. These dictate motion in the unit ellipse. The determination of these elements introduces the Fourier transform. Motion in the unit ellipse is related to motion in the unit circle through Kepler's equation. There appear to be two widely accepted methods of solving this equation. The first is through iteration. One presumes the values of P, T, and e, and then iterates by any of a wide variety of schemes to solve Kepler's equation at each of the epochs of observation. The great power of the Fourier transform approach to orbital computation arises through the well-known properties of the Fourier transform of Kepler's equation. As demonstrated in § II, solution of Kepler's equation at each epoch of observation is avoided. Hence the Fourier transform approach needs no preliminary information concerning T and e, and all elements, with the exception of the orbital period, may be computed directly from the Fourier transform of the observations.

The effects of observational noise are particularly suited to discussion in the transform domain. In the case of random observational uncertainty, the spectrum of the noise in the transform domain is frequency independent (white noise). It is beyond the scope of this investigation to consider the sources of nonrandom observational error, although it should be noted that spectral analysis of the noise is a useful tool for detecting the presence of nonrandom noise. Of particular interest are some of the techniques available in the transform domain for minimizing the effect of the noise, especially the optimal (Wiener) filtering technique. The implementation of such techniques is not included in this paper, as extensive discussions may be found elsewhere (see, e.g., Helstrom 1967).

The Fourier transform has been applied to the orbital analysis problem in the past, although the difficulties involved in the numerical computations seem to have yielded only specific realizations of the general form of the equations. The technique applied to a spectroscopic binary is known as the Wilsing-Russell solution (Russell 1902). While noting many of the benefits obtained through the use of the transform, Russell developed the solution for the lowest two harmonics (the minimum number to determine the orbital elements), noted that the computations were quite extensive, and indicated that the method of Lehmann-Filhés was much easier to compute. The work of Luyten (1935) again demonstrated that, in the limit of small eccentricities, the transform solution seemed quite desirable, and that the computations were not prohibitive. The discussion offered in § II*a* of this paper is simply the extension of the Wilsing-Russell solution to all frequencies and to develop an alternative method for determining the elements from the observed coefficients. The generalization to higher frequencies is quite useful for work with eccentricities larger than a few tenths. Quite surprisingly, there seems to be no equivalent to the Wilsing-Russell solution in general usage for visual binaries. Examination of the equations (24a)–(24d) is quite illuminating. The coefficients are quite nearly Thiele-Innes constants, the difference being the functions of the eccentricity, which are, in the case of the lowest frequency and lowest order, equal to unity. The Fourier series is an explicit representation of the systematic trends in observations. Hence these solutions offer no radical departure from familiar orbital determination methods.

The essence of the argument for the use of the Fourier transform is the availability of explicit predictions in the transform domain if Kepler motion is present. In configuration space, there appears to be only the equation for the observable quantity in terms of the orbital elements, and solution procedures seek a minimum discrepancy between observations and computed values through iterative improvement. In the transform domain, the Kepler hypothesis predicts every amplitude in the Fourier transform of the observations. The Fourier transform of the observations may be computed, and error estimators for each of the amplitudes may be determined by algorithms which do not presume Kepler motion. The solution procedure begins with computing orbital elements by requiring equality in as many amplitudes as there are unknown orbital elements. By using the general properties of the Fourier amplitudes, the choice for this solution can be made to include most of the available signal. All other amplitudes predicted by this Kepler orbit may be compared with the observational detection (or lack thereof) of amplitudes at these frequencies in order either to improve the first solution or to demonstrate its improbability. This comparison is limited only by the observational uncertainty. As the Fourier transform neither gains nor loses information, the same conclusion must be obtained in either configuration space or the transform domain. The desirability of the transform domain arises through analytic solution, explicit representation of the nature of the signal which must be present in the observational data, and error analysis based on model-independent error estimators.

II. SOLUTIONS

The method of solution in each of the four cases is essentially the same. Each time-dependent quantity is expressed as a Fourier series in the mean anomaly. The Fourier transform of the observable is expressed by

$$\boldsymbol{O}(t_i) = \sum_{n=0}^{\infty} a_n \cos(n\mathfrak{M}_i) + \sum_{n=1}^{\infty} b_n \sin(n\mathfrak{M}_i)\,, \tag{1}$$

where $\mathfrak{M}_i = (2\pi/P)(t_i - t_0)$, P is the period, t_i is the time of the ith observation, and t_0 is the observer's zero of time. The observer's mean phase $\mathfrak{M}$ and the mean anomaly M are related by the parameter Δ through the equation

$$M_i = \mathfrak{M}_i - \Delta\,, \tag{2}$$

where $M_i = (2\pi/P)(t_i - T)$, T is the time of periastron passage, and $\Delta = (2\pi/P)(T - t_0)$. Therefore,

$$\boldsymbol{O}(t_i) = \sum_{n=0}^{\infty} \alpha_n \cos(nM_i) + \sum_{n=1}^{\infty} \beta_n \sin(nM_i)\,, \tag{3}$$

where $\alpha_0 = a_0$, $\alpha_n = a_n \cos(n\Delta) + b_n \sin(n\Delta)$, and $\beta_n = b_n \cos(n\Delta) - a_n \sin(n\Delta)$. The determination of the parameters Δ fixes the difference between the observer's clock and the orbital clock, and hence the value of T.

The time-dependent functions of elliptic motion may also be expressed as Fourier series. In particular, much effort has been spent expressing these functions as series in the mean anomaly, with coefficients that are functions of the eccentricity. Cayley (1859) tabulated the coefficients for the expansions of various functions of elliptic motion through terms including the seventh power of the eccentricity. Jaranagen (1965) published tables including terms to the twentieth power of the eccentricity. Hence, the Fourier transform of the equation relating the observable and the functions of elliptic motion is

$$\sum_{n=0}^{\infty} \alpha_n \cos(nM_i) + \sum_{n=1}^{\infty} \beta_n \sin(nM_i)$$

$$= f(\text{orbital elements}) \sum_{n=0}^{\infty} F_n(e) \cos(nM_i) + g(\text{orbital elements}) \sum_{n=1}^{\infty} G_n(e) \sin(nM_i)\,. \tag{4}$$

Because of the orthogonality properties of the Fourier series, the above expression is the same as

$$\alpha_n = f(\text{orbital elements}) F_n(e)\,, \qquad \text{for } n = 0, 1, 2, \ldots \tag{5a}$$

and

$$\beta_n = g(\text{orbital elements}) G_n(e)\,, \qquad \text{for } n = 1, 2, \ldots. \tag{5b}$$

These equations are then solved for the orbital elements as a function of the observed a_n and b_n. The only approximations in the solution are the power series expansions for the F_n and G_n.

This method produces an infinite number of equations. Hence, the choice must be made either to solve the minimum number of equations exactly, or to perform a "least squares" or similar solution on many equations. The choice made in this work is to solve only the minimum number of equations. In particular, only the lowest-frequency equations are used, as one of the properties of the elliptic expansions is that each coefficient involves a power of the eccentricity one higher than the previous one. This implies that the majority of the signal due to orbital motion is to be found in the lowest-frequency components.

The general scheme for solving the set of equations is as follows. The set of equations may be reduced to a single expression that is an implicit function of the eccentricity which evaluates to zero. Because of the complexity of that expression, the choice is made to search numerically for the solution. Values of the eccentricity are tried until the sign of the residual changes. Once bracketed, the correct value may be found by standard interpolation algorithms. Because the elements ω and Δ are defined on the interval 0°–360°, some expressions involve a choice of sign. Solutions for each of the possible choices of sign are attempted. In all cases examined, the incorrect choice of sign either prohibited solving for the eccentricity or resulted in an imaginary orbital element.

The choice of notation in this paper follows that of Batten (1973). The various orbital elements are (a, e, i, ω, Ω, P, T, V_0, K). Furthermore, let ν denote the true anomaly, r/a denote the quotient radius, V denote the radial velocity, ρ denote the apparent separation, and θ denote the position angle. The variables F_n and G_n (and H_n, when necessary) are reserved for the coefficients of the various elliptic expansions. To avoid unnecessary symbols, the F_n and G_n are defined in each of the following sections independently of their definitions in the other sections. Finally, the choice is made to present the various equations in the form in which they are encoded for the computer.

a) The Radial Velocity Solution

In conventional notation, the orbit is characterized by

$$V = V_0 + K[\cos(u) + e\cos(\omega)]\,, \tag{6}$$

where $u = \nu + \omega$. Trigonometric substitution yields

$$V = V_0 + K\cos(\omega)\cos(\nu) + Ke\cos(\omega) - K\sin(\omega)\sin(\nu)\,. \tag{7}$$

The sine and cosine of the true anomaly are taken as

$$\cos(\nu) = F_0 + \sum_{n=1}^{\infty} F_n \cos(nM)\,, \tag{8a}$$

$$\sin(\nu) = \sum_{n=1}^{\infty} G_n \sin(nM)\,. \tag{8b}$$

The Fourier transform of the radial velocity data is taken to be

$$V = a_0 + \sum_{n=1}^{\infty} a_n \cos(n\mathfrak{M}) + \sum_{n=1}^{\infty} b_n \sin(n\mathfrak{M})$$

$$= a_0 + \sum_{n=1}^{\infty} [a_n \cos(n\Delta) + b_n \sin(n\Delta)] \cos(nM) + \sum_{n=1}^{\infty} [b_n \cos(n\Delta) - a_n \sin(n\Delta)] \sin(nM) . \tag{9}$$

A simplification involves noting that

$$F_0 = -e \tag{10}$$

exactly. Hence the equations are

$$V_0 = a_0 , \tag{11a}$$

$$F_n K \cos(\omega) = a_n \cos(n\Delta) + b_n \sin(n\Delta) , \tag{11b}$$

$$G_n K \sin(\omega) = a_n \sin(n\Delta) - b_n \cos(n\Delta) . \tag{11c}$$

The five unknowns in the solution are e, Δ, V_0, ω, and K.

The equations involved in the solution are those for $n = 0$, 1, and 2. The following results are valid for the general case $m = 2n$. The expressions for K and ω are rewritten as

$$K^2 = \frac{a_n^2 + b_n^2}{F_n^2 \cos^2(\omega) + G_n^2 \sin^2(\omega)} , \tag{12}$$

$$\tan(\omega) = \pm \frac{|F_n|}{|G_n|} \left(\frac{R_F^2 - R_{mn}}{R_{mn} - R_G^2}\right)^{1/2} , \tag{13}$$

where $R_F = F_m/F_n$, $R_G = G_m/G_n$, and $R_{mn} = (a_m^2 + b_m^2)/(a_n^2 + b_n^2)$. The elimination of all variables except the eccentricity yields

$$0 = \tan(\phi_m - 2\phi_n)[2R_{mn}(R_F - R_G) - R_F(R_F - R_G)^2] \mp \left(\frac{R_F^2 - R_{mn}}{R_{mn} - R_G^2}\right)^{1/2} [2R_{mn}(R_G - R_F) - R_G(R_G - R_F)^2] , \tag{14}$$

where $\tan(\phi_m) = b_m/a_m$ and $\tan(\phi_n) = b_n/a_n$. The solution for Δ is

$$\tan(n\Delta - \phi_n) = \frac{G_n}{F_n} \tan(\omega) . \tag{15}$$

The numerical solution of equation (14) should proceed normally. In practice, however, the term

$$\frac{R_F^2 - R_{mn}}{R_{mn} - R_G^2}$$

is greater than zero over such a tiny range of eccentricity that it is much easier to search for the zero crossings of the numerator and denominator, and then to evaluate equation (14) over the range of eccentricities remaining. This curiosity is understood when the expressions for R_F and R_G are examined. Long division yields

$$R_F \approx e(1 - \tfrac{5}{48}e^2 + \cdots) , \qquad R_G \approx e(1 - \tfrac{7}{48}e^2 + \cdots) .$$

These equations explicitly demonstrate the small "signal" associated with the element ω in the solution. The incorrect choice of sign in equation (14) prohibits solution.

b) The "Visual Binary" Orbit

The traditional equations to be solved are

$$\rho = r \cos(\nu + \omega) \sec(\theta - \Omega) , \tag{16}$$

$$\tan(\theta - \Omega) = \tan(\nu + \omega) \cos(i) . \tag{17}$$

A more convenient choice is the use of

$$\rho \cos(\theta - \Omega) = \frac{r}{a} [a \cos(\nu + \omega)] , \tag{18}$$

$$\rho \sin(\theta - \Omega) = \frac{r}{a} [a \sin(\nu + \omega) \cos(i)] . \tag{19}$$

The solution outlined by equations (13) and (14) of Monet (1977), while not incorrect, is less efficient that the one presented here. Expanding the trigonometric functions and reordering the equations yield

$$\rho \sin(\theta) = \left[\frac{r}{a}\cos(\nu)\right][a\cos(\omega)\sin(\Omega) + a\cos(i)\sin(\omega)\cos(\Omega)]$$

$$+ \left[\frac{r}{a}\sin(\nu)\right][-a\sin(\omega)\sin(\Omega) + a\cos(i)\cos(\omega)\cos(\Omega)]\,, \tag{20}$$

$$\rho \cos(\theta) = \left[\frac{r}{a}\cos(\nu)\right][a\cos(\omega)\cos(\Omega) - a\cos(i)\sin(\omega)\sin(\Omega)]$$

$$+ \left[\frac{r}{a}\sin(\nu)\right][-a\sin(\omega)\cos(\Omega) - a\cos(i)\cos(\omega)\sin(\Omega)]\,. \tag{21}$$

The Fourier transforms of $(r/a)\cos(\nu)$ and $(r/a)\sin(\omega)$ are expressed as

$$\left(\frac{r}{a}\right)\cos(\nu) = F_0 + \sum_{n=1}^{\infty} F_n \cos(nM)\,, \tag{22a}$$

$$\left(\frac{r}{a}\right)\sin(\nu) = \sum_{n=1}^{\infty} G_n \sin(nM)\,. \tag{22b}$$

Fourier transforms of the observations are taken as

$$\rho\cos(\theta) = a_0 + \sum_{n=1}^{\infty} a_n \cos(n\mathfrak{M}) + \sum_{n=1}^{\infty} b_n \sin(n\mathfrak{M})\,, \tag{23a}$$

$$\rho\sin(\theta) = c_0 + \sum_{n=1}^{\infty} c_n \cos(n\mathfrak{M}) + \sum_{n=1}^{\infty} d_n \sin(n\mathfrak{M})\,. \tag{23b}$$

The resulting equations are

$$a_n\cos(n\Delta) + b_n\sin(n\Delta) = aF_n[\cos(\omega)\cos(\Omega) - \cos(i)\sin(\omega)\sin(\Omega)]\,, \quad \text{for } n = 0, 1, 2, \ldots, \tag{24a}$$

$$-a_n\sin(n\Delta) + b_n\cos(n\Delta) = aG_n[-\sin(\omega)\cos(\Omega) - \cos(i)\cos(\omega)\sin(\Omega)]\,, \quad \text{for } n = 1, 2, \ldots, \tag{24b}$$

$$c_n\cos(n\Delta) + d_n\sin(n\Delta) = aF_n[\cos(\omega)\sin(\Omega) + \cos(i)\sin(\omega)\cos(\Omega)]\,, \quad \text{for } n = 0, 1, 2, \ldots, \tag{24c}$$

$$-c_n\sin(n\Delta) + d_n\cos(n\Delta) = aG_n[-\sin(\omega)\sin(\Omega) + \cos(i)\cos(\omega)\cos(\Omega)]\,, \quad \text{for } n = 1, 2, \ldots. \tag{24d}$$

The six unknowns are a, e, i, ω, Ω, and Δ.

The equations used in the solution are those for $n = 0$ and $n = 1$. The following is true for the equations for $n = 0$ combined with those for arbitrary n. Substitution yields

$$\tan(n\Delta) = \frac{c_0a_n - a_0c_n}{a_0d_n - c_0b_n}\,, \tag{25}$$

$$\frac{F_n}{F_0} = \pm\frac{a_n(a_0d_n - c_0b_n) + b_n(c_0a_n - a_0c_n)}{a_0[(a_0d_n - c_0b_n)^2 + (c_0a_n - a_0c_n)^2]^{1/2}}\,. \tag{26}$$

It is convenient to define

$$\alpha = a_n\cos(n\Delta) + b_n\sin(n\Delta)\,, \tag{27a}$$

$$\beta = -a_n\sin(n\Delta) + b_n\cos(n\Delta)\,, \tag{27b}$$

$$\gamma = c_n\cos(n\Delta) + d_n\sin(n\Delta)\,, \tag{27c}$$

$$\delta = -c_n\sin(n\Delta) + d_n\cos(n\Delta)\,. \tag{27d}$$

The expressions for the other elements of the orbit are

$$\tan(2\omega) = \frac{2F_nG_n[(\alpha\gamma)(\beta^2+\delta^2)+(\beta\delta)(\alpha^2+\gamma^2)]}{(\beta\gamma+\alpha\delta)[F_n^2(\beta^2+\delta^2)-G_n^2(\alpha^2+\gamma^2)]}, \tag{28}$$

$$\cos(i) = -\frac{[F_n^2(\beta^2+\delta^2)-G_n^2(\alpha^2+\gamma^2)]+\cos(2\omega)[F_n^2(\beta^2+\delta^2)+G_n^2(\alpha^2+\gamma^2)]}{[F_n^2(\beta^2+\delta^2)-G_n^2(\alpha^2+\gamma^2)]-\cos(2\omega)[F_n^2(\beta^2+\delta^2)+G_n^2(\alpha^2+\gamma^2)]}, \tag{29}$$

$$\tan(\Omega) = \frac{[\gamma G_n\cos(\omega)-\delta F_n\sin(\omega)]}{[\delta F_n\cos(\omega)+\gamma G_n\sin(\omega)]\sec(i)}, \tag{30}$$

$$a^2 = \frac{G_n^2(\alpha^2+\gamma^2)+F_n^2(\beta^2+\delta^2)}{[1+\cos^2(i)]F_n^2G_n^2}. \tag{31}$$

Equation (26) is to be searched as a function of the eccentricity. The ambiguity of sign originates with the choice of quadrant for $n\Delta$ in equation (25). The incorrect choice of sign prohibits an acceptable solution for the value of the eccentricity.

c) *The "Angles Alone" Orbit*

The "angles alone" solution is based on the equation

$$\tan(\theta-\Omega) = \tan(\nu+\omega)\cos(i). \tag{32}$$

A more useful form of that equation is

$$\tau_1+\tau_2\cos(2\nu)+\tau_3\sin(2\nu) = \tau_4\cos(2\theta)+\tau_5\cos(2\nu)\cos(2\theta)+\tau_6\sin(2\nu)\cos(2\theta), \tag{33}$$

where

$$\tau_1 = \cos(2\Omega)[1-\cos^2(i)],$$

$$\tau_2 = -2\sin(2\omega)\sin(2\Omega)\cos(i)+\cos(2\omega)\cos(2\Omega)[1+\cos^2(i)],$$

$$\tau_3 = -2\cos(2\omega)\sin(2\Omega)\cos(i)-\sin(2\omega)\cos(2\Omega)[1+\cos^2(i)],$$

$$\tau_4 = 1+\cos^2(i),$$

$$\tau_5 = \cos(2\omega)[1-\cos^2(i)],$$

$$\tau_6 = -\sin(2\omega)[1-\cos^2(i)].$$

The functions of the true anomaly are taken to be

$$\cos(2\nu) = \sum_{n=0}^{\infty} F_n\cos(nM), \tag{34a}$$

$$\sin(2\nu) = \sum_{n=1}^{\infty} G_n\sin(nM). \tag{34b}$$

The data are represented by

$$\cos(2\theta) = \sum_{n=0}^{\infty} a_n\cos(n\mathfrak{M})+\sum_{n=1}^{\infty} b_n\sin(n\mathfrak{M}), \tag{35a}$$

or

$$\cos(2\theta) = \sum_{n=0}^{\infty} \alpha_n\cos(nM)+\sum_{n=1}^{\infty} \beta_n\sin(nM), \tag{35b}$$

where

$$\alpha_n = a_n\cos(n\Delta)+b_n\sin(n\Delta), \qquad \beta_n = b_n\cos(n\Delta)-a_n\sin(n\Delta).$$

The product of two Fourier series is expressed as another Fourier series. In particular, let

$$\cos(2\theta)\cos(2\nu) = \sum_{m=0}^{\infty}\sum_{n=0}^{\infty}\alpha_m\cos(mM)F_n\cos(nM) + \sum_{m=1}^{\infty}\sum_{n=0}^{\infty}\beta_m\sin(mM)F_n\cos(nM)$$
$$= \sum_{n=0}^{\infty}\mathscr{A}_n\cos(nM) + \sum_{n=1}^{\infty}\mathscr{B}_n\sin(nM)\,, \tag{36a}$$

$$\cos(2\theta)\sin(2\nu) = \sum_{m=0}^{\infty}\sum_{n=1}^{\infty}\alpha_m\cos(mM)G_n\sin(nM) + \sum_{m=1}^{\infty}\sum_{n=1}^{\infty}\beta_m\sin(mM)G_n\sin(nM)$$
$$= \sum_{n=0}^{\infty}\mathscr{C}_n\cos(nM) + \sum_{n=1}^{\infty}\mathscr{D}_n\sin(nM)\,. \tag{36b}$$

Equations (36a) and (36b) serve implicitly to define $\mathscr{A}_n$, $\mathscr{B}_n$, $\mathscr{C}_n$, and $\mathscr{D}_n$. By equating the terms in each of the Fourier series, the following equations are produced:

$$\tau_1 + \tau_2 F_0 = \alpha_0\tau_4 + \mathscr{A}_0\tau_5 + \mathscr{C}_0\tau_6\,, \tag{37a}$$

$$\tau_2 F_n = \alpha_n\tau_4 + \mathscr{A}_n\tau_5 + \mathscr{C}_n\tau_6\,, \quad \text{for } n = 1, 2, \ldots, \tag{37b}$$

$$\tau_3 G_n = \beta_n\tau_4 + \mathscr{B}_n\tau_5 + \mathscr{D}_n\tau_6\,, \quad \text{for } n = 1, 2, \ldots. \tag{37c}$$

The five unknowns are e, i, ω, Ω, and Δ.

The set of equations (37a)–(37c) may be solved in the following manner. The eccentricity and Δ are involved in a rather complicated manner in the infinite series $\mathscr{A}_n$, $\mathscr{B}_n$, $\mathscr{C}_n$, and $\mathscr{D}_n$. Rather than attempt to decouple them, the solution proceeds by assuming values for e and Δ. Hence those sums may be evaluated over the finite frequency range of the measured a_n and b_n. For any two distinct nonzero frequencies i and j (usually 1 and 2),

$$(\tau_5/\tau_4) = \boldsymbol{A}/\boldsymbol{C}\,, \tag{38a}$$

$$(\tau_6/\tau_4) = \boldsymbol{B}/\boldsymbol{C}\,, \tag{38b}$$

$$(\tau_2/\tau_4) = [\alpha_i + \mathscr{A}_i(\tau_5/\tau_4) + \mathscr{C}_i(\tau_6/\tau_4)]/F_i\,, \tag{38c}$$

$$(\tau_3/\tau_4) = [\beta_i + \mathscr{B}_i(\tau_5/\tau_4) + \mathscr{D}_i(\tau_6/\tau_4)]/G_i\,, \tag{38d}$$

$$(\tau_1/\tau_4) = \alpha_0 + \mathscr{A}_0(\tau_5/\tau_4) + \mathscr{C}_0(\tau_6/\tau_4) - F_0(\tau_2/\tau_4)\,, \tag{38e}$$

where

$$\boldsymbol{A} = (F_i\mathscr{C}_j - F_j\mathscr{C}_i)(G_i\beta_j - G_j\beta_i) - (F_i\alpha_j - F_j\alpha_i)(G_i\mathscr{D}_j - G_j\mathscr{D}_i)\,,$$
$$\boldsymbol{B} = (F_i\alpha_j - F_j\alpha_i)(G_i\mathscr{B}_j - G_j\mathscr{B}_i) - (F_i\mathscr{A}_j - F_j\mathscr{A}_i)(G_i\beta_j - G_j\beta_i)\,,$$
$$\boldsymbol{C} = (F_i\mathscr{A}_j - F_j\mathscr{A}_i)(G_i\mathscr{D}_j - G_j\mathscr{D}_i) - (F_i\mathscr{C}_j - F_j\mathscr{C}_i)(G_i\mathscr{B}_j - G_j\mathscr{B}_i)\,.$$

The variables (i, ω, Ω) may then be calculated by means of

$$\cos^2(i) = \frac{1 - [(\tau_5/\tau_4)^2 + (\tau_6/\tau_4)^2]^{1/2}}{1 + [(\tau_5/\tau_4)^2 + (\tau_6/\tau_4)^2]^{1/2}}\,, \tag{39a}$$

$$\tan(2\omega) = -\frac{(\tau_6/\tau_4)}{(\tau_5/\tau_4)}\,, \tag{39b}$$

$$\cos(2\Omega) = (\tau_1/\tau_4)\frac{1 + \cos^2(i)}{1 - \cos^2(i)}\,. \tag{39c}$$

The above equations are functions of (τ_1/τ_4), (τ_5/τ_4), and (τ_6/τ_4). Hence the equations for (τ_2/τ_4) and (τ_3/τ_4) then define the correct choice for e and Δ. A particularly useful form for those equations is

$$\epsilon_1(e, \Delta) = (\tau_1/\tau_4) - (\tau_2/\tau_4)(\tau_5/\tau_4) - (\tau_3/\tau_4)(\tau_6/\tau_4) \tag{40a}$$

and

$$\epsilon_2(e, \Delta) = 4\frac{1 - [(\tau_5/\tau_4)^2 + (\tau_6/\tau_4)^2]^{1/2}}{1 + [(\tau_5/\tau_4)^2 + (\tau_6/\tau_4)^2]^{1/2}}[(\tau_5/\tau_4)^2 + (\tau_6/\tau_4)^2 - (\tau_1/\tau_4)^2] - [(\tau_2/\tau_4)(\tau_6/\tau_4) - (\tau_3/\tau_4)(\tau_5/\tau_4)]^2\,. \tag{40b}$$

In this form, the correct choice of (e, Δ) occurs when $\epsilon_1 = \epsilon_2 = 0$.

The preceding two-parameter search appears to be satisfactory. Most of the (e, Δ) space is uninteresting, as the values for (τ_1/τ_4), (τ_5/τ_4), and (τ_6/τ_4) require imaginary values for i, ω, or Ω. In the small remaining region of the space, the solution is found by mapping the curves $\epsilon_1 = 0$ and $\epsilon_2 = 0$. There are usually two intersections of these curves. One intersection is easily found, as the curves are "almost perpendicular" when they cross. This is the spurious solution. The interesting intersection is more difficult to find, as the curves lie very close to each other over a modest portion of the space. This "almost parallel" intersection may be found with suitable algorithms. With the correct values of e and Δ, the parameters of the orbit are found using equations (39a) and (39b). A more useful expression for equation (39c) is

$$\tan(2\Omega) = \pm\frac{(\tau_2/\tau_4)(\tau_6/\tau_4) - (\tau_3/\tau_4)(\tau_5/\tau_4)}{(\tau_2/\tau_4)(\tau_5/\tau_4) + (\tau_3/\tau_4)(\tau_6/\tau_4)} \frac{1}{1 - [(\tau_5/\tau_4)^2 + (\tau_6/\tau_4)^2]}, \tag{41}$$

where the sign is that chosen for the inclination. Finally, experience indicates that a search at fixed Δ is cheaper than a search at fixed eccentricity.

d) The "Separations Alone" Orbit

The equations

$$\rho = r\cos(\nu + \omega)\sec(\theta - \Omega), \tag{42}$$

$$\tan(\theta - \Omega) = \tan(\nu + \omega)\cos(i) \tag{43}$$

are combined to yield

$$\rho^2 = r^2[\cos^2(i) + \sin^2(i)\cos^2(\nu + \omega)]. \tag{44}$$

Further manipulation leads to

$$\rho^2 = \left(\frac{r}{a}\right)^2 \cos(2\nu)[\tfrac{1}{2}a^2\sin^2(i)\cos(2\omega)] + \left(\frac{r}{a}\right)^2 \sin(2\nu)[-\tfrac{1}{2}a^2\sin^2(i)\sin(2\omega)] + \left(\frac{r}{a}\right)^2[a^2 - \tfrac{1}{2}a^2\sin^2(i)]. \tag{45}$$

The Fourier expansions of the various functions of the ellipse are taken to be

$$\left(\frac{r}{a}\right)^2 \cos(2\nu) = \sum_{n=0}^{\infty} F_n \cos(nM), \tag{46a}$$

$$\left(\frac{r}{a}\right)^2 \sin(2\nu) = \sum_{n=1}^{\infty} G_n \sin(nM), \tag{46b}$$

$$\left(\frac{r}{a}\right)^2 = \sum_{n=0}^{\infty} H_n \cos(nM). \tag{46c}$$

When expressed in this manner, the infinite sums referred to in Monet (1977) are not needed. The separations and the times allow for the determination of the Fourier coefficients of

$$\rho^2 = \sum_{n=0}^{\infty} a_n \cos(n\mathfrak{M}) + \sum_{n=1}^{\infty} b_n \sin(n\mathfrak{M}) = \sum_{n=0}^{\infty} \alpha_n \cos(nM) + \sum_{n=1}^{\infty} \beta_n \sin(nM), \tag{47}$$

where

$$\alpha_n = a_n\cos(n\Delta) + b_n\sin(n\Delta), \qquad \beta_n = b_n\cos(n\Delta) - a_n\sin(n\Delta).$$

Equating the coefficients of each of the terms yields

$$\alpha_n = F_n[\tfrac{1}{2}a^2\sin^2(i)\cos(2\omega)] + H_n[a^2 - \tfrac{1}{2}a^2\sin^2(i)], \tag{48a}$$

$$\beta_n = G_n[-\tfrac{1}{2}a^2\sin^2(i)\sin(2\omega)]. \tag{48b}$$

The five unknowns are a, e, i, ω, and Δ.

The solutions use the equations for $n = 0, 1$, and 2. The following relations are valid for any two distinct nonzero frequencies n and m. Equations (7a) and (7b) reduce to

$$\beta_n/G_n = \beta_m/G_m, \tag{49}$$

$$\frac{\alpha_0 - a^2H_0}{F_0\cos(2\omega) - H_0} = \frac{\alpha_n - a^2H_n}{F_n\cos(2\omega) - H_n} = -\frac{\beta_m}{G_m\sin(2\omega)} = \tfrac{1}{2}a^2\sin^2 i. \tag{50}$$

Further manipulation produces the expressions

$$\tan(2\omega) = \frac{\beta_n}{G_n}\frac{(H_n F_m - H_m F_n)}{(\alpha_n H_m - \alpha_m H_n)}, \tag{51}$$

$$a^2 = \frac{\cos(2\omega)(\alpha_0 F_n - \alpha_n F_0) - (\alpha_0 H_n - \alpha_n H_0)}{\cos(2\omega)(H_0 F_n - H_n F_0)}. \tag{52}$$

The solution proceeds with the choice of a value for the eccentricity. Equation (49) relates Δ to the chosen eccentricity and to the a_n and b_n. In general, it yields two possible values for Δ. Equation (51) is then used to find each of the two possible values of 2ω for each of the possible values of Δ. The correct value of the eccentricity is the one which allows equation (50) to be satisfied. With the correct values of the eccentricity and 2ω, equation (52) gives the solution for a, and equation (50) then yields the value of the inclination. In practice, three of the four possible solutions require a or i to be imaginary, and may be discarded.

III. DETAILS OF IMPLEMENTATION

Many authors refer to a divergence in the Russell solution for eccentricities of $e > 0.6$, and hence limit their discussions to eccentricities much smaller than that value. It is unfortunate that a divergence which occurs in a related problem has been associated with a well-defined solution technique. Details of the divergence appear in Plummer (1918), but a summary of his arguments is relevant to the present discussion. The Fourier transform of a Kepler orbit does exist, and the coefficients are absolutely convergent for all $e < 1$. The problem arises in computational methods which reorder the expansion. A divergence is introduced when the Fourier expansion with coefficients that are power series in the eccentricity is reordered to be a power series with coefficients which are trigonometric functions. It is therefore necessary to compute the coefficients for each harmonic to some accuracy rather than to limit the series at some fixed power of the eccentricity for highly eccentric orbits. Recursive programming using the generating functions for the expansion coefficients provides an adequate solution to this problem. It should be noted that only the simple estimators in the previous sections made use of the form of the power series representation of the coefficients, and that the general solution procedure of equating coefficients of the Fourier series is valid for any eccentricity $e < 1$. An additional concern is the presence of observational uncertainty. Since the observed coefficients are not known to infinite precision, there is then some practical limit to the accuracy needed in the computation of the coefficients. The experience of Wolfe, Horak, and Storer (1967) indicated that plausible first orbits were obtained to $e \lesssim 0.8$ using only the first term in the expansions. Experience gained by the author indicates that observations rarely support significant detection of even the five lowest harmonics, and almost never as many as 10. The tabulations by Jaranagen supply coefficients to the twentieth power of the eccentricity, hence even the tenth harmonic can include five terms before the use of the generating functions is needed. In every case examined by the author, the analytic solution based on the lowest harmonics provided a preliminary orbit which was near the one obtained by iteration in configuration space, and the lack of precision for the expansion coefficients was insignificant when compared to the observational uncertainty.

The primary complication in implementation of the theory presented in § II is the difficulty in obtaining the Fourier coefficients. The difficulty arises through the very nonuniform sampling of typical astronomical data. The typical data for a visual binary is moderately well behaved, as complete revolutions are rarely missed, and hence the extensions of the fast Fourier transform (FFT) presented by Meisel (1978) may be considered. In the case of spectroscopic binaries, especially of short period, complete revolutions may be missed in a single observing run, and many revolutions may be missed between observing runs. The discussion by Meisel (1979) is relevant to these situations.

As a result of the rather limited computational facilities readily available to the author, a useful compromise algorithm was developed, although it is not optimal in the sense of minimum computing time or treatment of the nonuniformity of the sampling. The majority of systems to be investigated were of eccentricities sensibly smaller than unity, and a signal-to-noise ratio of the order of 100 or larger was unexpected. The properties of the expansion coefficients then indicate that only the first few Fourier coefficients will have significant amplitudes with respect to the noise. In addition, the Fourier components, while not linearly independent due to unequal sampling intervals, should be only weakly coupled, as the sampling of the observations is not usually locked to orbital phase.

A fitting function of

$$O(t_i) = \sum_{m=0}^{M} a_m \cos(m\mathfrak{M}_i) + \sum_{m=1}^{M} b_m \sin(m\mathfrak{M}_i)$$

(in the notation of § II), and

$$\chi^2(P, M) = \sum_{i=1}^{M} w_i[o_i - O(t_i)]^2,$$

where there are N observations o_i of weight w_i at time t_i, was adopted. The function is band-limited to M frequencies, as it is known that the harmonics above some limit (to be determined) must be dominated by noise, and hence a least-squares fit to the known functional dependence of the signal, would provide error estimators without the need to actually compute the amplitudes of each of the noise harmonics. In addition, the period is in general known to an approximate value before analysis begins, and hence the sampling of all possible orbital periods seems unnecessary.

As the Fourier components are expected to be almost linearly independent, initial analysis presumes M to be small (usually $M = 2$ is sufficient). This increases both speed of computation and numerical stability. Trial values of the period are assumed (and the least-squares fit to the amplitudes performed) until χ^2 is minimized. The assumption here is that the best estimator of the orbital period is that which minimizes the fit to the functional representation of Kepler motion. Since the uncertainty in the orbital period is usually small compared to the uncertainties in the coefficients, it is sufficient to take the error in the period from numerical differentiation of χ^2. At the best period, an orbit is computed to determine the eccentricity. This orbit serves to indicate whether M should be increased and the procedure redone.

The fitting procedure is usually successful for small values of M, as most data will not support fits (that is to say that numerical instabilities appear and prevent meaningful determination of Fourier coefficients) for more than four or five frequencies. Exceptionally accurate data, such as that available from radial-velocity spectrometers, may allow for determination of a few more coefficients. The numerical analysis is rapid, as it involves inversion of square matrices of dimension of the number of frequencies M, and not of order of the number of observations N, which may be quite large. The error estimators for the observed coefficients are supplied by the covariance matrix, which should be close to the expected one (diagonal elements all equal to σ^2, and all other elements zero). This is numerical verification that the Fourier coefficients are essentially linearly independent, given the data sampling, and that white noise is a good model for the observational uncertainty.

The first example is HR 6388, a well-observed system of moderate eccentricity ($\sim$0.6). Two orbits for this system were computed from the radial-velocity spectrometer data presented by Griffin and Emerson (1978). The period was assumed to be that given by Griffin and Emerson, 876.25 days, as it incorporates the older Lick data in the solution. These orbits are presented in Table 1 along with that given by Griffin and Emerson. The first orbit is that obtained by fitting only the lowest two harmonics (the Russell solution) to the data. This demonstrates that a crude approximation in the fitting function yields an orbit which is close to the final one. This is due to the very small linear interdependence of the Fourier harmonics in well, but not uniformly, sampled data. The large formal uncertainty estimators are caused by the appearance of a great deal of signal in χ^2 which is unaccounted for in the fit. The second orbit is based on a fit to six harmonics. The preliminary solution was iterated in the transform domain. Fitting more than six frequencies to the data serves no useful purpose, because the sixth harmonic is only 2.5 times larger than its uncertainty estimator and all higher harmonics will be even more poorly determined. This solution yields uncertainty estimators which are about 50% larger than those presented by Griffin and Emerson (1978). This discrepancy may be understood in the following manner. The value of χ^2 is used to determine the uncertainty of an observation of unit weight. A Kepler orbit of eccentricity near 0.6 is only poorly approximated by its lowest six harmonics. Hence the residuals from the band-limited representation may not be accurate estimators of the true observational uncertainty in cases of large eccentricity. The value of χ^2 should be computed from configuration space residuals in order to estimate the uncertainty of an observation of unit weight for highly eccentric orbits.

Further applications of the equations presented in § II were undertaken, and the following are typical examples of the orbital analysis produced. A well-observed spectroscopic binary of low eccentricities is HD 45088 (Griffin and Emerson 1975). The results of the analysis are presented in Table 2 with the elements derived by Griffin and Emerson. Despite the high accuracy of the observations, the small orbital eccentricity causes only the first three harmonics to have amplitudes larger than 3 times their formal errors. The orbital period was taken to be that given by Griffin and Emerson. Analysis according to the previous algorithm yields $P = 6.99185 \pm 0.00007$ days. A plot of the fit to the Fourier transform appears in Figure 1. A well-observed visual binary is ADS 1598 ($= \beta 513$). McAlister and DeGioia (1979) have observed this system with a speckle interferometer at KPNO; however, those data were not included in this analysis. The results are presented in Table 3. It should be noted that the squaring of the equations involved with the separations-alone and the angles-alone solutions introduces an uncertainty of 180° in ω, and hence the agreement of this element is also acceptable. As this was used for demonstration purposes, all observations were taken to be of unit weight. Subsequent reanalysis of the system using the normal places and weights of Heintz (1969) yields essentially similar results. Again it should be noticed that only a few orbital harmonics are significantly larger than their formal errors with this combination of somewhat larger eccentricity but with larger observational uncertainty. Also of interest is the conclusion that the angular data are of intrinsically better quality than the separations data, as can be seen by the uncertainty estimators for the elements that the separate solutions have in common. Heintz's period was assumed; however, the analysis procedure yielded a value of $P = 60.4 \pm 0.3$ years. Plots of the fits to the Fourier transform for the three orbits appear in Figure 1.

IV. CONCLUSIONS

The purpose of the equations presented in § II and the examples in § III was not simply to demonstrate that similar solutions are obtainable in both configuration space and the transform domain. The examples chosen were

Table 1

Orbits for the Spectroscopic Binary HR 6388

	M=2	M=6	Griffin & Emerson (1978)
K [km/sec]	6.20 (1.64)	4.94 (0.16)	4.79 (0.11)
e	0.70 (0.13)	0.616 (0.022)	0.609 (0.014)
ω [°]	111 (13)	106 (3)	103.0 (2.6)
T [MJD]	42407 (35)	42393 (4)	42389.4 (2.7)
V_o [km/sec]	-57.49 (0.16)	-57.58 (0.09)	-57.58 (0.07)
P [day]	876.25	876.25	876.25 (0.38)

() indicates 1 standard deviation.

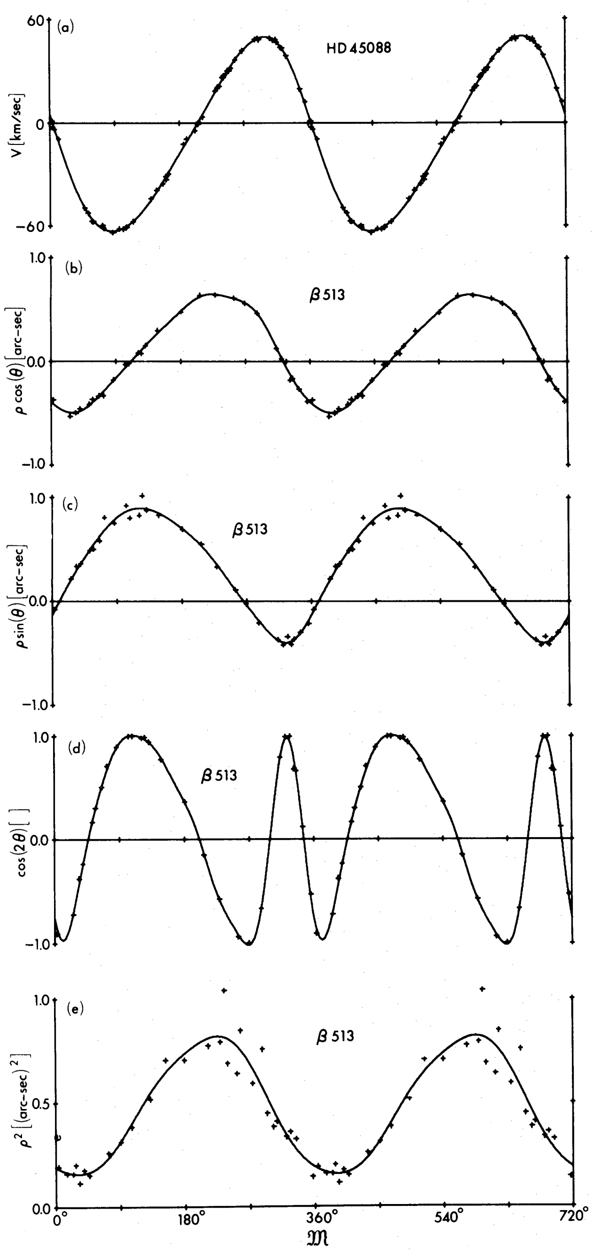

FIG. 1.—Sample data and their finite Fourier representations. In each part, the crosses are the observations and the solid line is the finite Fourier transform whose coefficients are presented in Table 2 or Table 3. Part (*a*) is the radial velocity of HD 45088. Parts (*b*)–(*e*) are $\rho \cos(\theta)$, $\rho \sin(\theta)$, $\cos(2\theta)$, and ρ^2 of β513.

Table 2

The orbit of the spectroscopic binary HD 45088

Fourier coefficients and their errors
(P=6.991868, t_0=MJD 40202.663)

V [km/sec] M=5

a_0= -8.41 (0.16)	
a_1= 11.88 (0.24)	b_1=-54.14 (0.23)
a_2= 1.91 (0.23)	b_2= -8.00 (0.26)
a_3= 0.00 (0.23)	b_3= -1.22 (0.26)
a_4= 0.10 (0.25)	b_4= -0.46 (0.25)
a_5= -0.22 (0.25)	b_5= 0.00 (0.25)

Orbital elements and their errors

Element	(this work)	(Griffin and Emerson)
V [km/sec]	-8.41 (0.16)	-8.40 (0.15)
e	0.149 (0.005)	0.150 (0.004)
K [km/sec]	56.54 (0.23)	56.55 (0.21)
ω [degrees]	78.6 (1.7)	77.6 (1.4)
T [MJD]	40202.68 (0.03)	40202.663 (0.029)
P [day]	6.991868 (assumed)	6.991868 (0.000065)

systems where observational uncertainty is small and where there is little doubt that the systems are in Kepler orbits. Rather, the analysis is the cornerstone for more detailed investigations of systems that are more poorly understood. The question of detecting unseen companions was addressed by Monet (1978). This demonstrated that the Fourier transform approach yielded analytic solution with uncertainty estimators for all elements, whereas configuration space techniques must make many, possibly profound, assumptions to arrive at a solution, and error analysis is a much more poorly defined process. The discussion of the detection of small eccentricities was presented by Monet (1979*a*). Here the treatment of the observational noise in the transform domain seems to yield better estimators for significance of detection. This work confirms the conclusions presented by Luyten (1935). The question of detection of apsidal motion was discussed by Monet (1979*b*), and a larger sample of data will be

Table 3

Orbits of the visual binary β513

Fourier coefficients and their errors
(P=60.44, t_0=1900.0)

ρcos(θ) [milli-arc-sec] M=5		ρsin(θ) [milli-arc-sec] M=5	
a_0=-122 (7)		c_0=-329 (13)	
a_1= 428 (10)	b_1=-362 (9)	c_1= 424 (19)	d_1= 443 (17)
a_2= 78 (10)	b_2= -25 (9)	c_2= 49 (18)	d_2= 76 (17)
a_3= 19 (10)	b_3= -3 (9)	c_3= -5 (18)	d_3= 20 (17)
a_4= -2 (9)	b_4= 12 (10)	c_4= -3 (16)	d_4= 14 (19)
a_5= -8 (8)	b_5= 0 (10)	c_5= -3 (16)	d_5= 3 (18)
1000cos(2θ) [ ] M=6		**ρ² [milli-(arc-sec)²] M=3**	
a_0= -89 (10)		a_0= 481 (18)	
a_1= 204 (15)	b_1= 578 (13)	a_1=-285 (27)	b_1=-176 (25)
a_2= 41 (14)	b_2=-556 (14)	a_2= -16 (27)	b_2= 10 (25)
a_3= 223 (14)	b_3=-401 (13)	a_3= 12 (26)	b_3= 10 (25)
a_4= 209 (13)	b_4=-138 (15)		
a_5= 131 (13)	b_5= -7 (15)		
a_6= 38 (13)	b_6= 32 (14)		

Orbital elements and their errors

Element	(ρ,θ)	(ρ alone)	(θ alone)	(Heintz)
a [arc-sec]	0.650 (0.018)	0.655 (0.034)		0.653
e	0.360 (0.015)	0.390 (0.066)	0.344 (0.006)	0.346
i [degrees]	22.0 (5.3)	26.8 (8.2)	20.4 (2.8)	22.8
ω [degrees]	355 (14)	161 (25)	175.9 (6.1)	4.5
Ω [degrees]	74 (13)		71.2 (5.6)	64.2
T [year]	1904.6 (0.3)	1904.4 (1.5)	1904.0 (0.3)	1964.78 [1904.34]
P [year]	60.44 (assumed)	60.44 (assumed)	60.44 (assumed)	60.44

examined for such motion by Monet (1980). Here again, the Fourier approach readily yields solutions and uncertainty estimators where classical techniques seem less desirable. Questions concerning detection of orbital motion in systems showing intrinsically variable stellar velocities are readily discussed in the transform domain, as the known properties of the transform of Kepler motion should be distinguishable from other sources of variation in velocity. In similar fashion, changes in velocity due to blending and eclipse effects should be distinguishable from true orbital motion.

The analysis of highly eccentric systems requires an algorithm different from that given in § III. The large number of harmonics with significant amplitudes is not well treated by the simple approximations made in that algorithm, and its use seems limited to systems with eccentricities of about 0.7 or less. The use of algorithms based on the fast Fourier transform, such as those developed by Meisel, should be considered. Despite the large number of harmonics included in such a solution, iteration is readily accomplished as there is no need to solve Kepler's equation for each of the epochs of observation, as must be done in configuration space algorithms.

It appears that there is no convenient alternative to iterative improvement of solutions with modest to large eccentricity. Experience indicates that the analytic solution using the lowest harmonics provides a preliminary solution which appears to be very close to the final one, as expected from signal-to-noise arguments. In this respect, there are a few distinct advantages of iteration in the transform domain. The iteration yields more information than simply the decrease of χ^2. The residuals of the expected and observed Fourier coefficients may be monitored in addition to the traditional (configuration space) residuals. In addition, noise-filtering algorithms available in the transform domain are available to include the effects of noise in the criterion for goodness of fit. The effect of iterative improvement on the orbital elements should be small, as the signal is known to be decreasing in the higher harmonics, but the noise remains constant (in the limit of white noise). Indeed, any large change in the orbital elements in the iteration process should cause concern about the validity of the assumption of Kepler motion. The preferred solution should include both configuration space and transform space iteration in an effort to provide internal tests of significance, as each minimizes a different quantity, but both should yield essentially the same solution if the hypothesis of Kepler motion and random noise is valid.

The Fourier transform solutions have many desirable properties. They treat both spectroscopic and visual binaries with the same formalism, and therefore, it is hoped, with the same systematic errors. This is of prime concern when combined solutions are attempted. These solutions require no preliminary estimator for the orbital elements. There is no need for a linearized form of the equations for motion. There is no need for normal places. The solutions identify the nature of the signal due to Kepler motion, and this signal is readily traced through the solution procedure to indicate the well- and poorly-defined orbital elements. The Fourier coefficients are well defined for all eccentricities, and hence no different scheme is needed in the limit of either small or large eccentricity. Uncertainty estimators are available for all elements of orbital motion based on model-independent determinations of the uncertainties in the observational data.

Additional advantages arise from the partial solutions available for visual binaries. The solutions in separations alone and angles alone provide an additional check on the quality of the combined solution. Each of the separate solutions has no reference to the other coordinate, as they both are solved without a preliminary orbit. The generalization for solutions in the orthogonal coordinates, X or Y, alone is readily derived from the equations in § II*b*, and need not be presented here. These solutions were intentionally chosen to refer to the square of the coordinate, or twice the angle, as many varieties of optical interferometers are subject to an ambiguity of 180° in angle determinations. These solutions should be immune to such ambiguities. The only uncertainty introduced by such a choice is an ambiguity of 180° in the longitude of periastron passage. A particularly interesting application of the angles-alone solution is for visual binaries of essentially the same magnitude, which causes an occasional ambiguity of 180° in the determined position angle. The angles-alone solution should yield the correct orbital period as well as the orbital elements with no need to presume which of the data are in error by 180° in position angle.

Because of the known structure of the amplitudes of the Fourier transform of Kepler motion, the algorithm presented in the previous section is moderately stable against changes in observational weight. In a configuration space iteration, the minimum is a strong function of the assigned weights, as the only quantity that is examined is the weighted sum of the square of the residuals. Hence a disagreement on the weights of the observations may cause a large difference in derived orbital elements. The solution in the transform domain appears to be more stable through the fit to the functional representation of Kepler motion. A sine curve cannot readjust its curvature to come arbitrarily close to a particular high weight observation that is significantly different from the sense of the rest of the observations. An ellipse which is allowed to change its eccentricity is capable of such changes in curvature. The fitting of the Fourier coefficients is best thought of in terms of the properties of the orthogonality integral which is used to derive the value of the coefficient,

$$a_n = \frac{2}{\pi}\int_0^{2\pi} \cos(n\mathfrak{M})O(\mathfrak{M})d\mathfrak{M} \approx \frac{2}{N}\sum_{i=1}^{N} \cos(n\mathfrak{M}_i)O(\mathfrak{M}_i)\,.$$

Hence the Fourier coefficients represent integrals over all data of functions of fixed curvature and are correspondingly less sensitive to a single observation.

In the final analysis, it is a matter of convenience as to whether the orbit is computed in configuration or transform domain. The Fourier solutions developed in the preceding sections appear to offer significant advantages over traditional iteration in configuration space. The conclusions of thorough analysis in either domain must be the same, owing to the information-preserving properties of the Fourier transform. It is not apparent that current configuration space algorithms are at, or can be brought to, the level of sophistication offered by transform domain algorithms. Ideally, both configuration space and transform domain situations should be attempted, as this offers unparalleled sensitivity to sources of noise or non–Keplerian phenomena in a particular set of observations. The cost of the additional computations seems small when compared with the cost of telescope time.

I would like to express my appreciation to those who were kind enough to offer critical comments on this work in the years since the preliminary version of this paper was circulated. I would also like to acknowledge computer time made available by Dr. K. M. Cudworth, and in the early phases, by Dr. L. M. Hobbs. The encouragement expressed in this project by Drs. Cudworth, P. O. Vandervoort, R. H. Miller, and W. F. van Altena is greatly appreciated. Special thanks are offered to E. Mondello and T. Weisflog.

This work was supported in part by the National Science Foundation.

REFERENCES

Batten, A. H. 1973, *Binary and Multiple Systems of Stars* (New York: Pergamon), p. 7.
Cayley, A. 1859, *Mem. R.A.S.*, **29**, 191.
Goldstein, H. 1950, *Classical Mechanics* (Reading: Addison-Wesley), p. 107.
Griffin, R. F., and Emerson, B. 1975, *Observatory*, **95**, 23.
———. 1978, *Observatory*, **98**, 14.
Heintz, W. D. 1969, *Astr. Ap.*, **1**, 249.
Helstrom, C. W. 1967, *J. Opt. Soc. Am.*, **67**, 297.
Jaranagen, M. P. 1965, *Astr. Papers*, **18**, 1.
Luyten, W. J. 1935, *Pub. Astr. Obs. U. Minn.*, **2**, 53.
McAlister, H. A., and DeGioia, K. A. 1979, *Ap. J.*, **228**, 493.
Meisel, D. D. 1978, *A.J.*, **83**, 538.
Meisel, D. D. 1979, *A.J.*, **84**, 116.
Monet, D. G. 1977, *Ap. J.* (*Letters*), **214**, L133.
———. 1978, *Ap. J.* (*Letters*), **223**, L101.
———. 1979*a*, *Pub. A.S.P.*, **91**, 95.
———. 1979*b*, *Pub. A.S.P.*, **91**, 218.
———. 1980, in preparation.
Plummer, H. C. 1918, *An Introductory Treatise on Dynamical Astronomy* (Cambridge: University Press), p. 46.
Russell, H. N. 1902, *Ap. J.*, **15**, 252.
Wolfe, R. H., Horak, H. G., and Storer, N. W. 1967, *Modern Astrophysics*, ed. M. Hack (New York: Gordon Breach), p. 251.

David G. Monet: Kitt Peak National Observatory, P.O. Box 26732, Tucson, AZ 85726